RAPID DETECTION OF MALARIA ANTIGEN IN HUMAN WHOLE BLOOD USING A HANDHELD LAB-ON-CHIP DEVICE

by

Charles Christopher Stemple

A Document Submitted to the Faculty of the

BIOMEDICAL ENGINEERING GRADUATE INTERDISCIPLINARY PROGRAM

In Partial Fulfillment of the Requirements
For the Degree of

MASTER OF SCIENCES

In the Graduate College of

THE UNIVERSITY OF ARIZONA

2011 STATEMENT BY AUTHOR

This report has been submitted in partial fulfillment of requirements for an advanced degree at The University of Arizona and is deposited in the University Library to be made available to borrowers under rules of the Library.

Brief quotations from this report are allowable without special permission, provided that accurate acknowledgment of source is made. Requests for permission for extended quotation from or reproduction of this manuscript in whole or in part may be granted by the head of the major department or the Dean of the Graduate College when in his or her judgment the proposed use of the material is in the interests of scholarship. In all other instances, however, permission must be obtained from the author.

SIGNED: Charles Christopher Stemple

Charles Christopher Stemple

APPROVAL BY REPORT DIRECTOR

This report has been approved on the date shown below:

J. Y. Yoon

Dr. Jeong-Yeol Yoon

8/30/11

Date

Table of Contents

List of Figures

List of Tables

Abstract

Malaria is a human infectious disease that affects around 250 million people each year. Primarily found in regions of Africa, Asia, and South America, malaria is typically caused by the protozoa *Plasmodium falciparum*, and results in symptoms ranging from high fever to death. The most common detection methods currently consist of ELISA, PCR, and blood film smears; however, each of these methods requires a full laboratory environment for proper utilization, with assay times ranging from 2-8 hours. In this study, a novel handheld detection device based on the properties of immunoagglutination will be modified to detect malaria in human whole blood through histidine-rich protein 2 (HRP-2), an antigen expressed only by *P. falciparum*. HRP-2 antibodies are covalently attached to 920 μm carboxylated polystyrene nanoparticles, which are mixed with the target human whole blood in a lab-on-chip testing environment. Using a 640 nm LED and avalanche photodiode pair, the sample is illuminated and forward light scatter caused by immunoagglutination of the HRP-2 antigen to the antibodies present on the nanoparticles is measured. The final device is compact, battery powered, low-cost, and capable of detecting HRP-2 antigens in human whole blood with a detection limit of 1 pg/mL and an assay time of approximately 8 minutes. The device represents a significant improvement in assay time over current malaria detection methods at a relatively low cost.

Section 1

Introduction

1.1 – Malaria Background

1.1.1 – Introduction and History

Malaria is a human parasitic disease that results in a variety of symptoms depending on its severity, ranging from chills and headaches to anemia, acute kidney failure, and death. Although not a common condition in developed nations, malaria remains a common and serious condition throughout parts of Africa, Asia, and South America. Malaria may very well be a condition that is as old as humanity itself, with written accounts matching its common characteristics dating as far back as Chinese medical writings in 2700 BC. Additional references to the then-unnamed "sickness" that resulted in fever and death were recorded in various parts of the world up until 1740, when it was given the formal name of malaria. Its name was given by H. Walpole, derived from the Italian expression "mal'aria" for "bad air", due to the observation that the disease was transferred through airborne means (Desowitz, 1991).

The parasitic nature of malaria was first discovered by Charles Louis Alphone Laveran in 1880. A French army surgeon, Laveran was treating a malaria-stricken soldier when he observed parasites in his blood, a fact later confirmed by French immunologist Pierre Paul Emile Roux. In 1886, Italian neurophysiologist Camillo Golgi reported that there were at least two different forms of the disease, with symptoms differing

depending on the type. Lastly, around 1897, British officer Ronald Ross was the first to observe that malaria could be transmitted through mosquito bites (Cox, 2010).

1.2.1 – Causes and Symptoms

Malaria results from infection by eukaryotic protozoa of the genus *Plasmodium*, which invade the bloodstream and infect red blood cells. The disease originates in *Anopheles* mosquitoes, where certain species of *Plasmodium* reside within the salivary glands of carrier mosquitoes. When a carrier mosquito withdraws a blood meal from a human, the parasites are passed into the bloodstream and infect an initial batch of red blood cells. The parasites will then differentiate over the course of 48-72 hours and begin infection of new red blood cells. Incubation times vary depending on *Plasmodium* species, with symptoms showing as quickly seven days after initial infection but potentially taking up to thirty days or more (Heussler, 2006).

Malaria can be grossly classified by severity into two categories – uncomplicated and severe. Uncomplicated malaria is rarely fatal, and is typically characterized by headaches, chills, increased sweating, nausea, vomiting, and achiness. Physical effects may include mild jaundice, an enlarged spleen and/or liver, and increased respiratory rate. In some cases, these symptoms occur in waves, with each series of symptoms lasting six to ten hours before receding for up to several days; these kinds of attacks are infrequently observed, however. The symptoms of a severe infection are far less general, and include high fever, anemia due to hemolysis, low blood pressure (often the result of cardiovascular collapse), metabolic acidosis, acute respiratory distress

syndrome (ARDS), and in some cases, a range of neurological conditions including unconsciousness, seizures, or coma. Severe malaria infections can often lead to organ failure and death if not treated quickly and properly (Miller, 2002).

1.3.1 – Biology and Species

Plasmodium is part of the protest group *Apicomplexa*, which are spore-forming, unicellular, and exist exclusively as parasites. They possess a unique cone-shaped projection of their cell membrane, known as the apical complex, which is instrumental in penetrating and infecting the host cell.

The lifecycle of a malarial infection occurs in three stages – the mosquito stage, the hepatic stage, and the blood stage. As previously mentioned, malaria originates in A*nopheles* mosquitoes and are prepped for human infection in the mosquito stage. Initially, male and female gametocytes, or parasite gametes formed by meiosis, combine to form zygotes within the mosquito. These zygotes mature into ookinetes, which then penetrate the mosquito's midgut in order to take up residence under the outer gut lining. Here, the ookinetes mature further into oocysts, which develop and eventually rupture, releasing infectious sporozites that move into the mosquto's salivary glands (Tripet, 2008).

Upon blood contact with a human host, anywhere from 5-200 sporozites will be transferred by the mosquito. These sporozites will travel to the liver and infect hepatic cells, where they will develop and eventually rupture, releasing merozites while

destroying the red blood cell host. These merozites will continue to multiply in the liver, eventually re-infecting new red blood cells using their apical complexes; the parasite will then shed its apical complex and become a trophozite, which is the activated form of malaria found in the red blood cell cytoplasm. The trophozite stage is also referred to as the "ring" stage, due to their physical appearance in a blood smear detection test (Pouvelle, 2000). As the trophozites feed on the hemoglobin of host cells, they will increase in size considerately to around 15µm in diamter, developing into schizonts which will replicate their DNA multiple times before segmenting into anywhere from 15-20 new merozitic cells. Thus, the infection will spread, and some merozites will eventually mature into gametocytes that can be extracted by feeding mosquitoes, bringing the malarial lifecycle full-circle (Pouniotis, 2004). Figure 1 summarizes the infectious lifecycle of *Plasmodium* parasites.

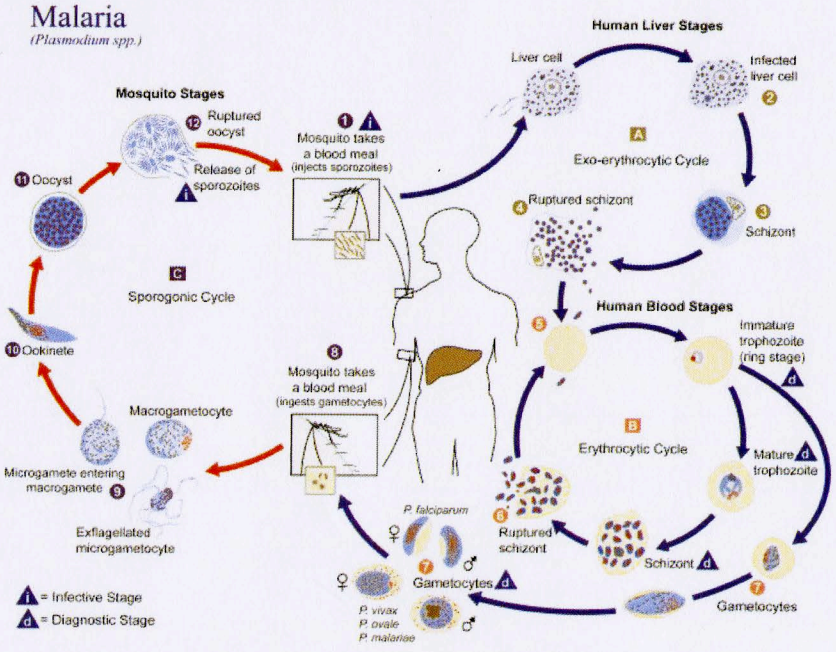

Figure 1 – *Plasmodium* lifecycle. (CDC, 2010)

Although there are approximately 200 known species of *Plasmodium*, only eleven are known to be infectious to humans, and four are known to cause malaria. The four species that cause malaria are *Plasmodium falciparum*, *Plasmodium malariae*, *Plasmodium ovale*, and *Plasmodium vivax*. *P. malaria, P. ovale,* and *P. vivax* are responsible for cases of uncomplicated malaria, and thus, represent mild forms of the disease which are typically non-deadly and easily curable, whereas *P. falciparum* causes severe malaria and is responsible for 90% of all malaria-related deaths (Bain, 2009) Whereas *P. falciparum* and *P. malariae* have incubation times of less than 30 days, *P. ovale* can remain dormant in the liver for up to two years before causing symptoms, and *P. vivax* can take up to four years. Each of the malaria-causing species follows similar infection patterns and lifecycles, but are distinguishable under a microscope due to subtle physical characteristics. These differences will be further discussed in Section 1.2.3 – Peripheral Blood Smears.

1.4.1 – Incidence

According to the World Health Organization (WHO), there are anywhere from 200-300 million cases of malaria per year resulting in approximately 1 million deaths annually. A majority of these deaths occur in children under 5 years of age, or adults over 60 years. Pregnant women have a higher susceptibility to *P. falciparum*, and as a result, up to 14% of infected mothers will give birth to children with low birth weight, further decreasing the infant's chance of survival (WHO, 2010).

Malaria occurs most frequently in central Africa, south Asia, and South America; according to the Center for Disease Control (CDC), 35 countries in these areas account for 98% of all malaria-related deaths, 30 of which are located in Africa alone. Further, the CDC has calculated that approximately half the world's population (around 3.3 billion) lives in regions with a risk of malaria infection. The disease is most prevalent in regions high in heat and humidity; in fact, at temperatures below 68° F, *P. falciparum* is unable to complete its growth cycle, thus preventing it from becoming transmissible. Among infectious diseases, malaria is the second leading cause of death in Africa behind HIV/AIDS, and is the fifth leading cause of disease-related death worldwide (CDC, 2010). The incidence of malaria around the world is shown in Figure 2.

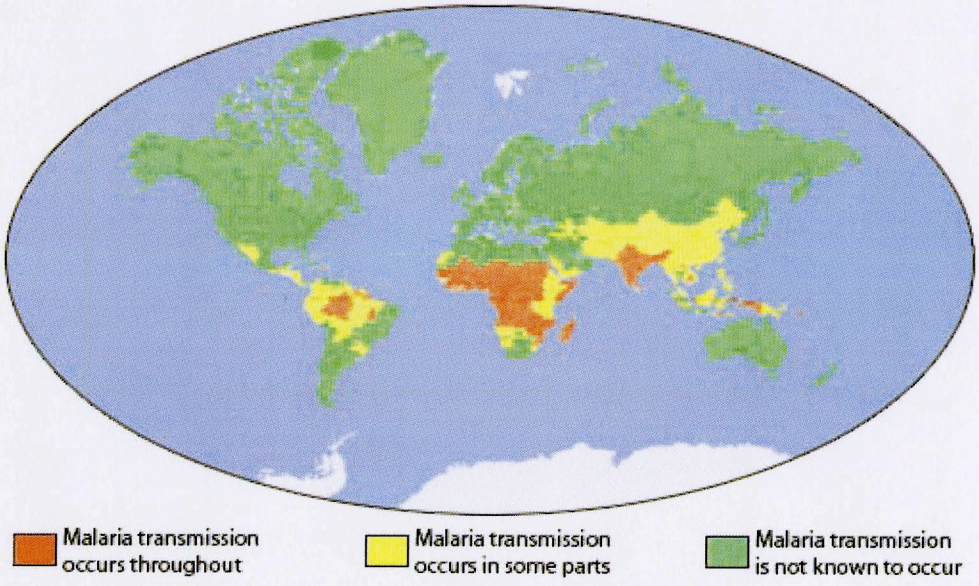

Figure 2 – Malaria occurrences throughout the world. (CDC, 2010)

1.2 – Current Detection Methods

1.2.1 – Peripheral Blood Smear

The current "gold standard" for malaria detection is the blood film, also known as a peripheral blood smear. In a blood smear, a blood sample is removed from the patient and a drop is placed on a standard glass microscope slide and then analyzed under a microscope to determine parasite counts and species. There are two types of smears – thin and thick smears. In a thick smear, a drop of the target blood is placed on the center of a microscope slide with a cover slip on top; in a thin smear, second spreader slide is used to spread the blood down the length of the slide, the purpose of which is to spread the cells in the blood far enough apart to identify and count. Thick smears are performed to determine if any *Plasmodium* parasites are present in the sample; the larger volume (as opposed to a thin smear) makes a thick smear over ten times more sensitive, and thus, much easier to detect the present of any parasites (Warhurst, 1996). However, what thick films gain in sensitivity, they lose in specificity; the physical appearance of the parasites are distorted by large blood volumes, which makes the thin smear ideal for determining the species of *Plasmodium* present.

The average observed detection limit of thick blood smears is around 50,000 trophozites/mL, with a thin smear detection limit of 50,000,000 trophozites/mL or higher (Moody, 2000). Blood smears are considered to be the gold standard for *Plasmodium* detection due to its ability to accurately identify both an active infection as well as the type of species present with the same experimental setup. However, blood

smears require individuals trained in distinguishing between *Plasmodium* species; the species are distinguishable based on the unique ring-shaped structures that their membranes take on in the trophozite stage. As illustrated in Figure 3, discerning differences between the various *Plasmodium* species at a microscopic level is very difficult. Standard protocol requires that at least 200 separate visual fields must be analyzed prior to reporting a result. This, in addition to the standard staining procedures, results in assay times around 2-8 hours in length, depending on the number of personnel available for analysis (Stauffer, 2009).

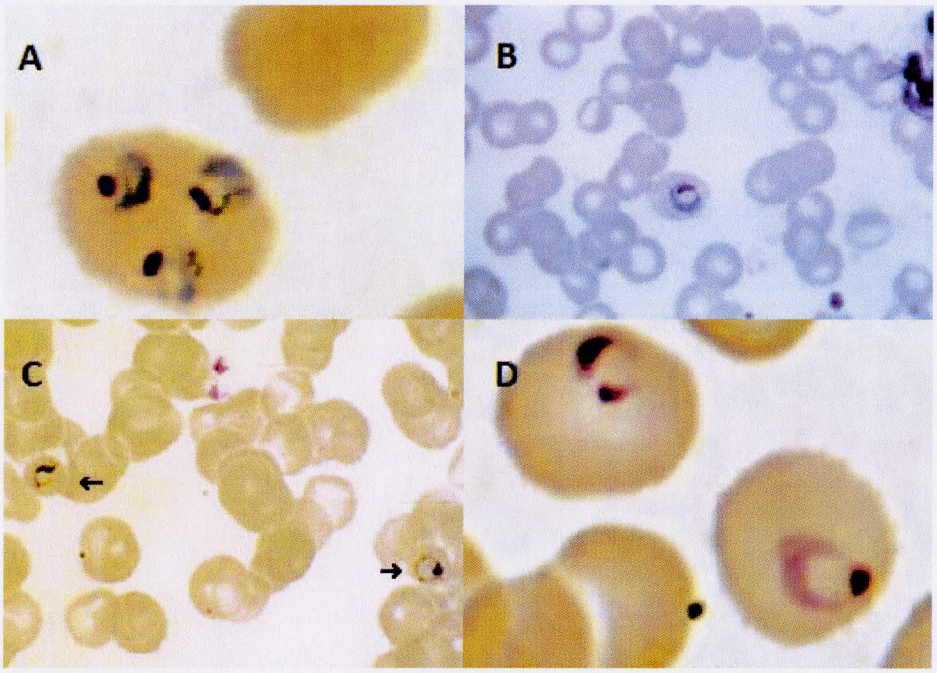

Figure 3 – Microscopy of *Plasmodium species*. A) *P. falciparum* B) *P. ovale* C) *P. malariae* D) *P. vivax*. (Keas, 1999)

1.2.2 – ELISA

A popular alternative to blood smears in malaria detection is the enzyme linked immunosorbent assay (ELISA). The technique is used to identify antibodies or antigens in a sample, and thus requires at least one antibody specific to the target. In a typical ELISA test, the sample is introduced to a multi-well microtiter plate with a capture antibody immobilized to the bottoms of the wells. A washing phase follows; then, a second detection antibody bound to an enzyme is introduced to the samples. Lastly, a substrate is added to the samples, and the enzyme converts the substrate into a detectable form (Crowther, 2001). Using a antigen specific to *P. falciparum*, the ELISA assay has a detection limit as low as 18 trophozites/mL and a specificity of 100% (Sure Bio-Diagnostics, 2009). Including sample preparation time, typical ELISA assay times are on the order of 2-3 hours.

1.2.3 – PCR

Polymerase chain reaction (PCR) is a DNA amplification technique that can also be used to detect for malaria. PCR is based on the concept of thermal cycling, or repeated cycles of heating and cooling periods, in order to promote DNA replication. Double-stranded DNA is exposed to high temperatures (above 90° C) min order to promote DNA melting, which causes the strands to separate. Short primer sequences that are complementary to the 3' end of the strands are introduced to the solution, and free nucleotides will being to build complementary strands to the previously denatured

double-stranded DNA. This process is repeated in order to generate multiple copies of the sequence of interest (Johnston, 2006). Previous studies have revealed that PCR has a *P. falciparum* detection limit ranging from 470-1200 trophozites/mL with 100% specificity (Mangold, 2005). PCR has a slight longer assay time than ELISA, taking around 4-5 hours to produce detectable concentrations of *P. falciparum* sequences.

1.3 – Detection by Immunoagglutination

1.3.1 – Overview

A relatively new means of pathogen detection is known as the particle immunoagglutination assay. Like the previously described methods, immunoagglutination is capable of pathogen detection in a biological sample matrix, but has the potential for significantly faster assay times with a simpler procedure while maintaining comparable detection limits.

The basis of immunoagglutination relies on the use of latex particles for detection. Antibodies, either monoclonal or polyclonal, are conjugated with sensitized latex particles, which typically vary in size from 100 μm to 10 nm; particles must typically be a minimum of 50 μm in order to be easily viewed under a microscope (Gella, 1991). The antibody-particle complex is then introduced to the target sample; in theory, the target will specifically bind to the antibodies present on the latex particles, forming a larger complex that can be detected through a variety of different means (Molina-Bolivar, 2005). Figure 4 illustrates the basic concept of immunoagglutination.

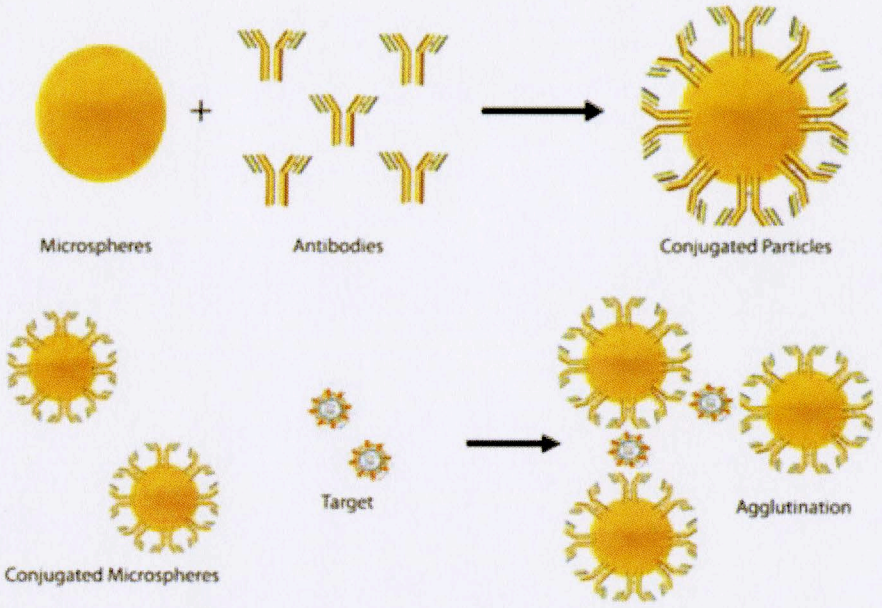

Figure 4 – Standard particle immunoagglutination assay.

1.3.2 – Mie Scattering

One sensing method that can be used to detect for the presence of immunoagglutination is optical light scattering based off the Mie principle (Equation 1).

$$\frac{I}{I_o} = \frac{1+cos^2\theta}{2R^2}\left(\frac{2\pi}{\lambda}\right)^4\left(\frac{n^2-1}{n^2+2}\right)^2\left(\frac{d}{2}\right)^6 \quad (1)$$

where I = scattering intensity, I_o = incident light intensity, θ = scattering angle, R = distance to the particle, λ = wavelength, n = refractive index, and d = diameter of a particle. Developed by German physicist Gustav Mie in the 1930s, the Mie principle presents a set of solutions to Maxwell's equations that approximate the light scatter caused by particles. Mie scattering is accurate for particles that are larger than the wavelength of the scattered light, as particles that are significantly smaller than the

wavelength of the incident light scatter light based off the Rayleigh principle (Kerker, 1969). Mie scattering and how it differs from Rayleigh scattering can be observed in Figure 5.

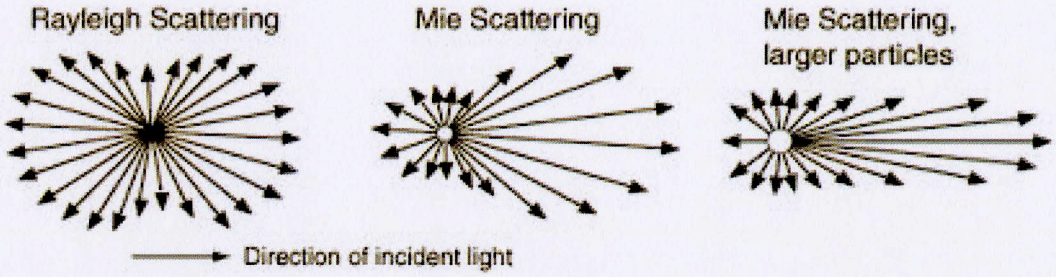

Figure 5 – Comparison of Rayleigh and Mie scattering.

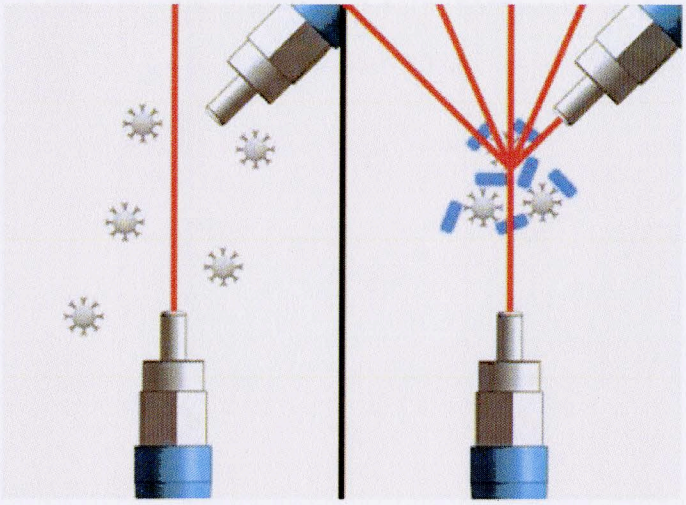

Figure 6 – Visualization of immunoagglutination-induced light scatter; the incident beam (bottom) does not scatter due to a lack of complexes (left), but will scatter in the presence of antibody-particle-target complexes.

Mie scattering can be used to detect the presence of immunoagglutination by illuminating a sample containing antibody-particle complexes with a fixed light source and measuring the change in light scatter that results from the increased size of the

antibody-particle-target complex. The light scatter created by immunoagglutination is visualized in Figure 6.

1.3.3 – Lab-on-Chip Diagnostics

A problem inherent to nearly all classical methods of pathogen detection is the need for a facility in which to perform the necessary diagnostics. Blood smears require the use of a high-powered microscope, which are typically sensitive to motion and vibration; ELISA requires storage methods for the various antibodies and enzymes involved with the process as well as a plate reader for analyzing the wells; and PCR requires not only storage for the DNA primers and fragments needed for amplifications, but also a thermocycler to heat and cool the samples in order to promote DNA replication. In recent decades, lab-on-chip technology has sought to integrate multiple laboratory functions into small, channeled chips that are typically no larger than a few inches. Further, lab-on-chip devices can be manufactured from a variety of materials, including glass, polydimethylsiloxane (PDMS), and various metals and ceramics. Lab-on-chip devices offer many potential advantages over standard laboratory environments, including significantly decreased space requirements, faster assay/analysis times, lower sample volumes, increased thermal control due to shortened diffusion distances (typically on the order of millimeters), and increased productivity due to the ease of running parallel experiments (Oosterbroek, 2003)

1.4 – Objectives

1.4.1 – Rapid Portable Detection Method for Malaria

As previously mentioned, although current malaria detection methods are both sensitive and specific, they possess characteristics that limit their usefulness in field studies, such as the use of expensive microscopy equipment, lack of portability due to the need for large laboratory environments, diagnostic times that may take several days (including sample transport), and requiring personnel trained in the use of all the aforementioned equipment. Given that a majority of clinical malaria cases take place in underdeveloped countries that typically lack proper medical facilities, there exists a need for a portable, inexpensive, and quick method for diagnosing malaria.

Combining the principles of latex particle immunoagglutination, Mie scattering, and lab-on-chip diagnostics, this study will focus on the development of a handheld pathogen detection device for use in the rapid diagnosis of malaria in human whole blood samples. Such a device will be battery powered and its form factor will allow it to be carried by any average person, and thus, can be carried to just about any location in order to diagnose samples. Further, in order to be clinically relevant, it will be able to detect parasites in human whole blood samples with a minimal amount of sample processing. The entire device will be relatively low cost and easily reproduced, and compared to other detection methods, will be user-friendly without requiring specific training.

Section 2

Methods and Materials

2.1 – Experimental Overview

The main focus of the experimental procedure is to determine the optimal procedure for detecting pathogens in human whole blood, verify that the chosen antibodies bind specifically to target malaria antigens, and validate the handheld device's ability to detect for immunoagglutination of malaria antigens to latex nanoparticle-antibody complexes.

2.2 – Handheld Device

2.2.1 – Physical Construction

The handheld's frame was designed by Hyuck-Jin Know and Scott Angus of the University of Arizona's biosensor laboratory using SolidWorks 2009. The form factor is 9" L x 7.0625" W x 1.75" D and weighs approximately 3 lbs. The body is constructed of black acrylonitrile butadiene styrene (ABS) plastic, and rapid-prototyped using a Statasys Dimension 1200ES printer. The face contains an LCD screen and five buttons, which comprise the primary user interface, displaying light scatter levels and allowing the user to calibrate the device. There are two ports on either side of the device, a female Type-B USB port and a female +9V DC input, both of which can be used to power and/or charge the device. Lastly, the bottom of the device features a removable tray that accepts a 3" L x 1" W microfluidic chip, in which the sample and antibody-particle complexes are analyzed (Kwon, 2010). The final device is shown in Figure 7.

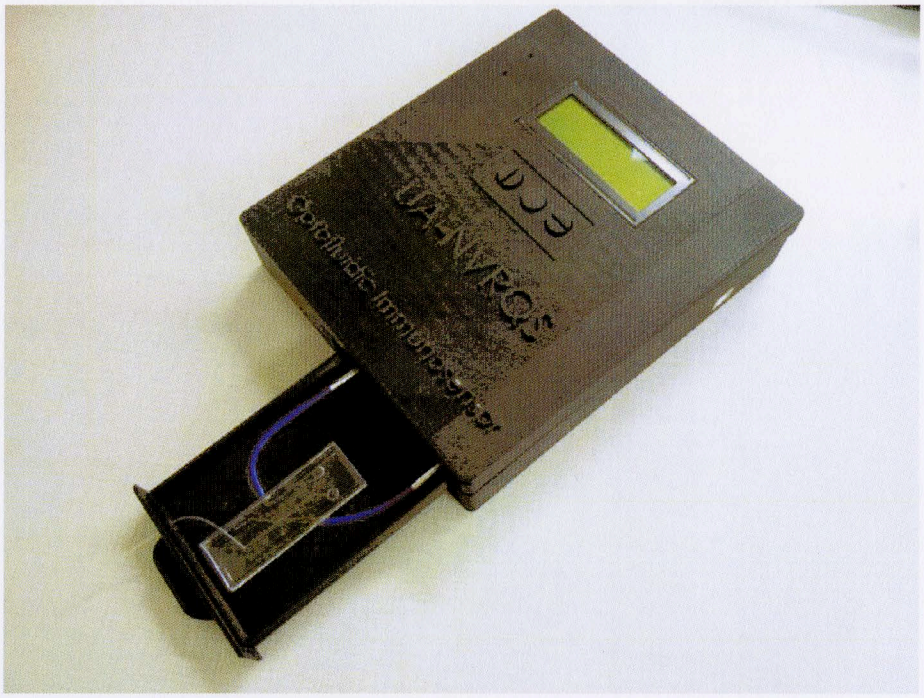

Figure 7 – Completed handheld detection device, with microfluidic tray removed.

2.2.2 – Electronics

The primary purpose of the electronics in the handheld system is to convert light scatter readings into a quantifiable metric for detecting immunoagglutination. There are six primary components to the electronics, which are detailed in Table 1; the major components are labeled in Figure 8.

Table 1 – Overview of handheld electronic components.

Component	**Description**	**Input Type**	**Output Type**
LED/Photodiode Pair	Illuminates sample with light and records forward scatter	640 nm (red) light	Current (mA)
Differential Op-Amp Circuit	Convert current output of photodiode into voltage	Current (mA)	Voltage (V)
Arduino Duemilanove	Microcontroller circuit that converts output for display on LCD screen	Voltage (V)	Voltage (V)

LCD Display	Displays light scatter levels in numeric form	Voltage (V)	Text (Numbers)
4.7V Lithium Battery	Allows device to function without a plug-in power supply	n/a	Voltage (V)
+5V/USB Power Board	Converts battery output to +5V and allows for charging via USB cable	Voltage (V)	Voltage (V)

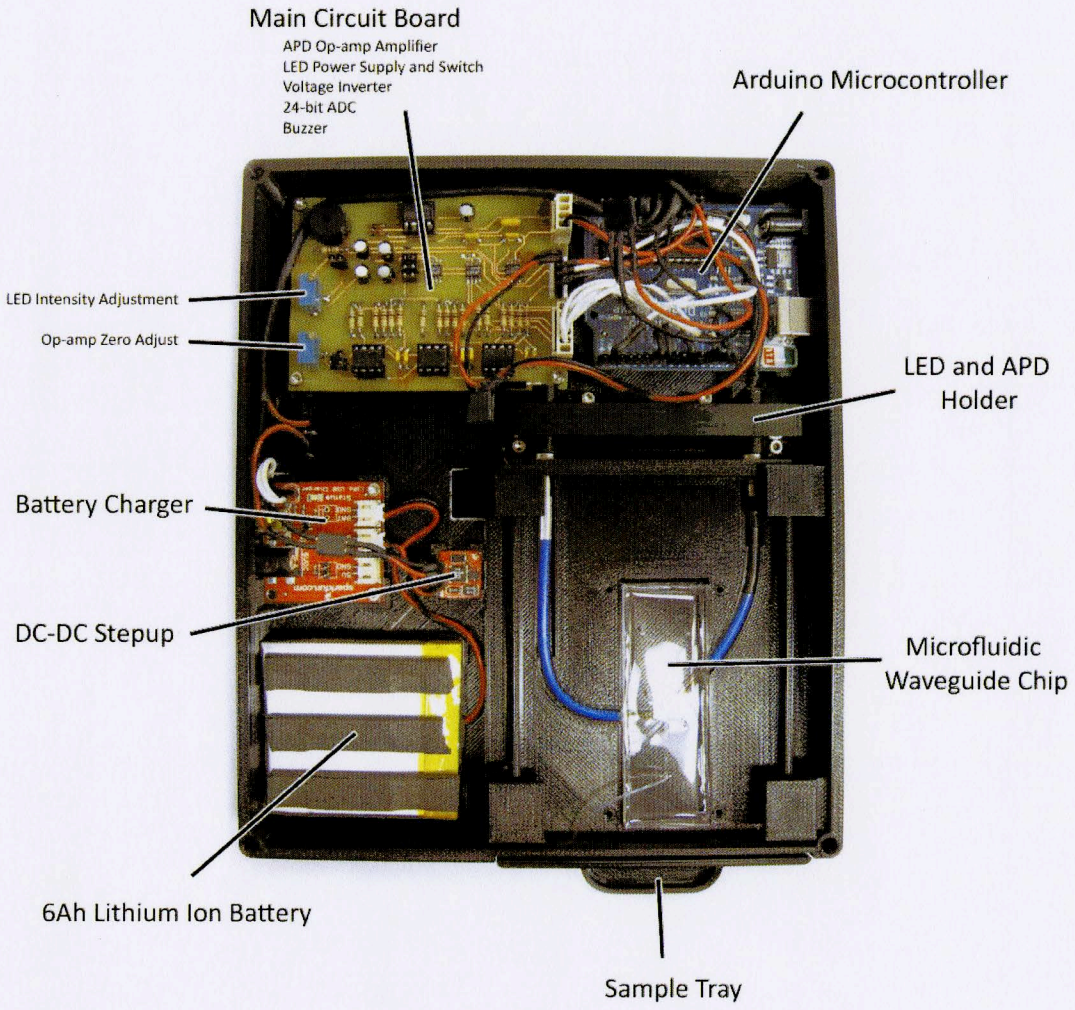

Figure 8 –Inside view of device with electronics labeled.

With the exception of the differential op-amp circuit, all of the electronics components are off-the-shelf parts available at any reputable electronics supplier.

The op-amp circuit is designed with a series of transimpedance amplifiers, the purpose of which is to convert a current signal into a voltage signal. This is necessary due to the fact that a photodiode outputs a current signal, and the Arduino only accepts voltage inputs. The LED driver is also integrated into the amplifier board, the purpose of which is to generate a constant light output from the LED. The schematic for the main board is shown in Figure 9, the final assembled board is shown in Figure 10, and the complete bill of materials is shown in Table 2.

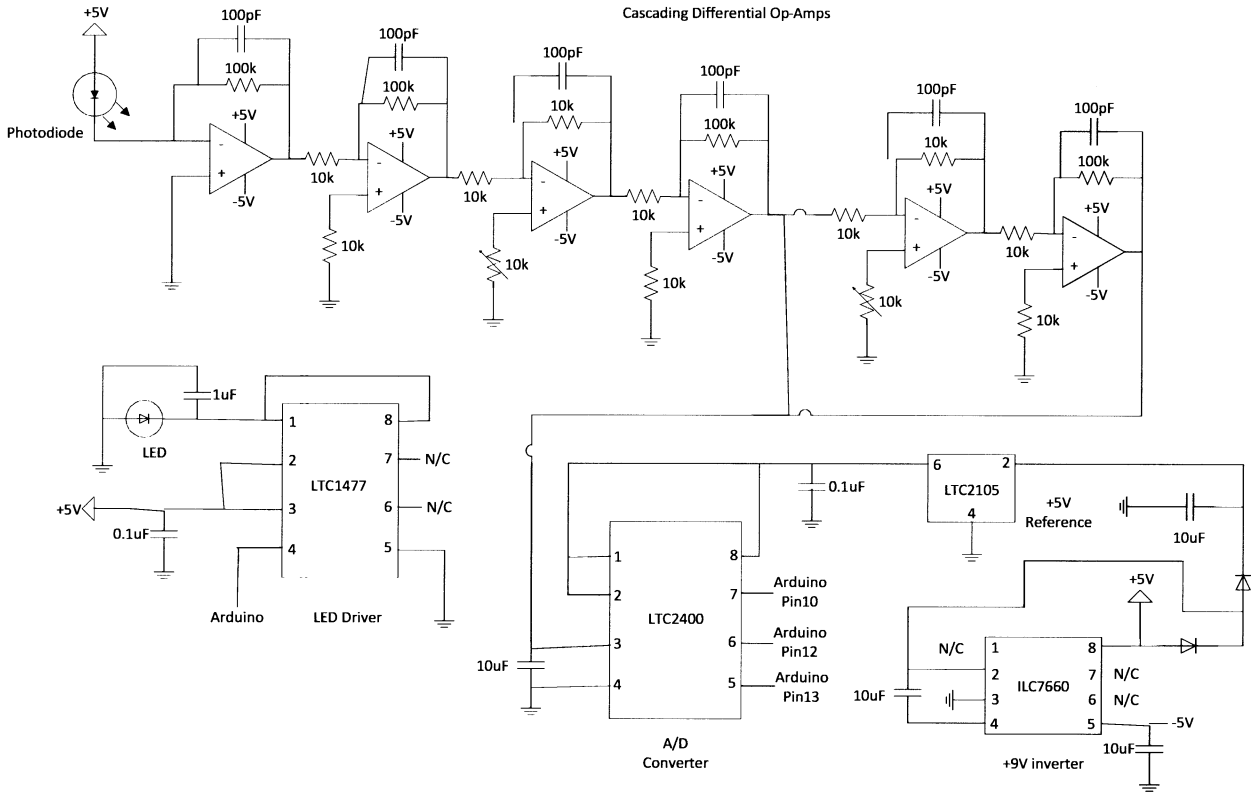

Figure 9 – Amplifier circuit and LED driver schematic.

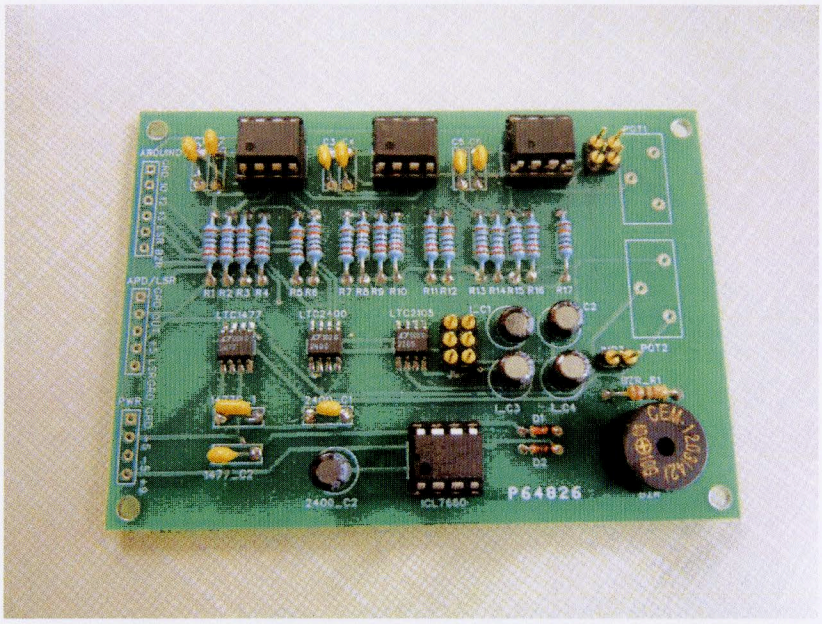

Figure 10 – Final assembled amplifier board.

Table 2 – Main board bill of materials.

Item No.	Qty	Ref Des	Description	Part #
1	1	LT1021	LT1021 5V Reference	LT1021DCS8-5#PBF-ND
2	1	LT2400	LTC2400 24 bit ADC	LTC2400CS8#PBF-ND
3	1	LT1477	LTC1477 Switch	LTC1477CS8#PBF-ND
4	6	C1-C6	100pF Capacitor	BC2657CT-ND
5	4	I_C1 - I_C4	10uF Capacitor	P975-ND
6	2	1477C1, 2400C1	0.1 uF Capacitor	399-4266-ND
7	3	OPA1-OPA3	IC Socket - 8 pin DIP	A24807-ND
8	3	OPA1-OPA3	TL082A Amplifier	296-1781-5-ND
9	1	BZR	Buzzer	102-1153-ND
10	12	R1-R4; R7-R10; R13-R16	10kΩ Resistor	RNF14FTD10K0CT-ND
11	5	R5-R6; R11-R12; R17	100kΩ Resistor	RNF14FTD100KCT-ND
12	1	BZR_R1	100Ω Resistor	CF14JT100RCT-ND
13	1	1477_C2	1uF Capacitor	BC1157CT-ND
14	1	7660	ICL7660 Voltage Converter	ICL7660CPAZ-ND
15	1	Headers	Terminal Headers	SAM1111-32-ND
16	2	POT1-POT2	10kΩ Potentiometer	3296W-103LF-ND

The operational amplifier cascade consists of six total stages, four of which are set up as gain stages, and two of which are zero adjust stages. Each gain stage has a gain of 10, with an overall circuit gain of 10,000 amps/volt, as the photodiode output is on the order of several nanoamps. The two zero adjust stages are used to calibrate the voltage output of the circuit through the use of 10 kΩ potentiometers which are user-adjustable through holes in the face of the handheld. The LT1021 is used to provide a stable +5V reference to the circuit, and helps maintain consistent light emission from the LED. The LTC2400 analog-to-digital converter allows for communication with the Arduino microcontroller board. The LTC1477 is a high side switch for controlling the LED. The ICL7660 outputs a fixed -5V output in order to power the negative rails of the op-amps. Lastly, the aforementioned Arduino microcontroller board converts the voltage output of the amplifier cascade to a digital signal that can be read by the LCD in order to display the amount of forward light scatter as an integer value.

The optical detection portion of the electronics consists of a 640nm (red) LED and an avalanche photodiode. There are three primary factors that led to the using an LED/photodiode pair – cost, availability, and previous studies. LEDs and photodiodes are inexpensive, easily replaced, a have small form factors. Although laser diodes and photomultiplier tubes are viable and potentially more sensitive alternatives, it is believed that a laser diode would be too directional for scatter-based detection, and photomultiplier tubes are significantly larger than photodiodes. Photodiode/LED pairs were also readily available through most major electronics suppliers. Lastly, red light

was chosen based off its performance compared to blue (470 nm) and ultraviolet (375 nm) light. Mie scattering simulations by You et al. observed the amount of light scatter difference between singlet particle models (in which only a single particle is bound to an antigen) and triplet models (in which three particles are bound to a single antigen) over a range of scatter angles. At the optimal scattering angle of 45°, ultraviolet produced the greatest scatter change, and blue produced the least amount of change. However, for angles $\pm$ 5° from optimal, there is a significant roll-off in the intensity curve; this could affect the stability of readings if the scatter angle were to change. Although red light didn't yield as high of a change as ultraviolet did, its intensity curve was flatter. Thus, red light was chosen because it offered the best compromise between light intensity change and reproducibility (You, 2011). The referenced Mie scattering simulations are shown in Figure 11.

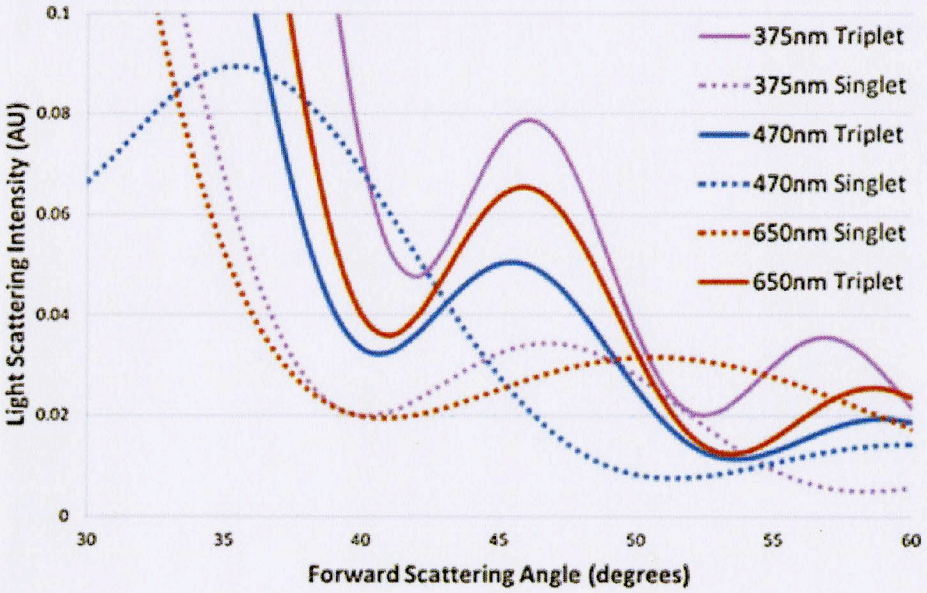

Figure 11 – Mie scattering simulations for red, blue, and ultraviolet light in both singlet and triplet forms.

2.2.3 – Microfluidic Chip

The microfluidic chip was originally designed by Brian Heinze of the University of Arizona's biosensor laboratory; it features a Y-channel design with two wells for inserting the target and antibody-particle complexes into the test channel, waveguides for accepting fiber optic cables, and a port at the end of the Y-channel that can accept a syringe for mixing the sample and evacuating the channels. The chip is constructed from PDMS, and has a form factor of 3" L x 1" W x 0.25" D. The chip layout is detailed in Figure 11.

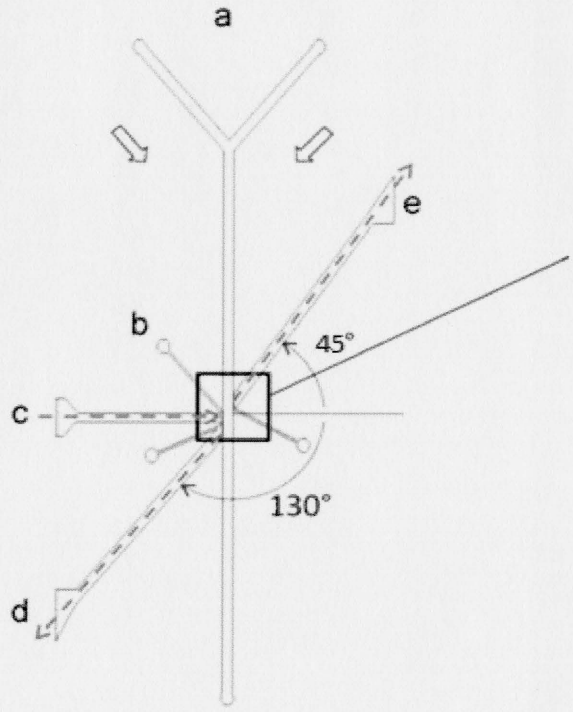

Figure 12 – Microfluidic test chip. a) Two inlets for administration of target antigens and nanoparticles. b) Waveguide fill ports. c) Incident waveguide, connected to the 640 nm LED. d) Back scatter waveguide (not used for this experiment). e) Forward scatter waveguide.

The chips are fabricated from a silicone master mold, which was created through photolithography combined with deep reactive ion etching (DRIE). To minimize loss during etching, a 6 μm thick photoresist (AZ 4620) was used as the silicon etching mask. C_4F_8 and SF_6 combined with O_2 were used for the passivation and etching steps. PDMS is poured into the mold and cured for one hour in a convection oven. Peeling the PDMS from the mold exposes the Y-channel, which is then bonded to a second PDMS through oxygen plasma treatment. The channels measure 1 mm wide by 100 μm in depth, with the waveguide channels measuring 750 μm wide by 100 μm in depth. The waveguide channels are designed to accept 100 μm diameter optic fiber cables sourced from Ocean Optics. The waveguide fill ports allow for the waveguide channels to be filled with microscope immersion oil Type A, with a refractive index of 1.515 (Nikon, 2010). A syringe in combination with Teflon tubing was used to deliver the oil; this same combination was also connected to the end of the Y-channel in order to pull the samples from the wells and mix them in the central channel (Heinze, 2010). The completed assembly with fiber optic cables is shown in Figure 12.

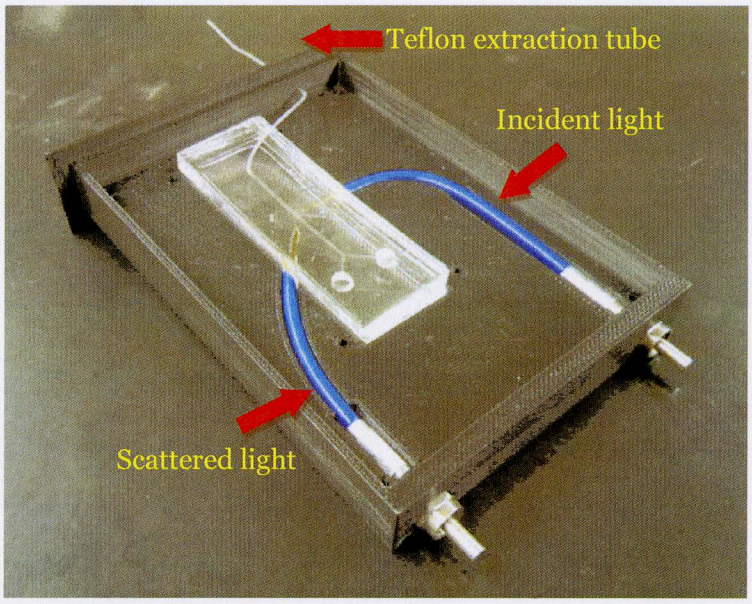

Figure 13 – Completed microfluidic detection assembly. The upper-right fiber optic cable delivers the incident light from the 640nm LED, with the lower-left cable receives the forward-scattered light from the sample and delivers it to the photodiode. The teflon tube near the top of the picture is connected to a syringe in order to mix the sample and empty the channel.

The forward scattering waveguide lies at an angle of 45° relative to the incident waveguide; this allows for scattered light collection anywhere from 40° to 70° relative to the incident angle. As previously observed by Heinze et al, the optimal angle for detecting forward scatter is 45°, based on both Mie scattering simulations and experiments for the detection of *E. coli* in liquefied lettuce samples (Heinze, 2011).

2.3– HRP-2 Antigen Preparation

Due to the high cost of acquiring and culturing live strains of malaria, recombinant antigens were chosen as the target for this study, which are non-infectious and suitable for use in a Biosafety Level-2 level laboratory. Specifically, histidine-rich protein 2 (HRP-2) recombinant antigens were chosen, which were acquired from Merdian Life Science, Inc. (Meridian Life Sciences, 2011). HRP-2 is a water-soluble protein specific to *P. falciparum*, and has been successfully detected in several rapid diagnostic tests over the past decade (Kakkilaya, 2003). Shipped from Meridian Life Sciences in a concentration of 6.65 mg/mL, the samples were first diluted to 1 mg/mL using a 20 mM carbonate buffer with a pH of 9.6, using 0.1% sodium azide as a preservative. Then, the antigens were serially diluted down to a minimum concentration of 1 pg/mL; the experiment was designed to detect for HRP-2 antigens ranging in concentration from 1 pg/mL to 100 μg/mL.

2.4 – Nanoparticle Preparation

Carboxylated polystyrene nanoparticles, high in acid content (15% acrylic acid) with a mean diameter of 920 nm in diameter, were chosen for this malaria study due to their success in previous immunoagglutination experiments (Kwon, 2010). A pair of monoclonal antibodies specific to HRP-2 were obtained, one designed for capture with the second designed for detection (Meridian Life Science, 2011). The monoclonal

antibody pair was covalently attached to the nanoparticles according to a procedure written by the Bangs Laboratories. The nanoparticles were first suspended in a 2-(N-morpholino)ethanesulfonic acid (MES) activation buffer ($C_6H_{13}NO_4S$, 50mM, pH 6.0, Sigma-Aldrich). The particles were washed through centrifuge at 9.9g for 15 minutes followed by removal of and resuspension in MES; this was repeated two times. 1-ethyl-3-(3-dimethylaminopropyl) carbodiimide (Fluka Analytical, Sigma-Aldrich) was then added to the nanoparticle suspension to serve as the primary linker between the antibodies and the particles. The suspension was then mixed constantly at room temperature for 15 minutes. Two additional washing periods followed, in which the particles were centrifuged for 22 minutes at 12g and resuspended in a coupling polymerase buffer solution or PBS (50mM, pH 7.4, Sigma-Aldrich). Next, a total of 7.6 µL of antibodies at a concentration of 1 mg/mL were added to the solution (3.8 u= µL of each monoclonal antibody) in PBS coupling buffer; this volume should theoretically result in 100% coverage of the particles, but as observed by Yoon, only covers 30-50% of the particles in practice (Yoon, 2008). The antibody concentration is calculated using Equation 2:

$$S = \frac{6C}{pD} \qquad (2)$$

where S is the concentration required for total saturation, and 6C/p is the surface area to mass ratio based on a nanoparticle diameter, and D is the nanoparticle

diameter (You, 2011). The solution is then mixed overnight on a rocker at 4°C. Three additional washing periods followed, with 22 minutes of centrifuge at 12g followed by resuspension in PBS. After the third washing period, the solution was resuspended in hydroxylamine (40mM with 1% bovine serum albumin [BSA], Sigma-Aldrich, and mixed constantly at room temperature for 30 minutes. The solution was mixed one more time and resuspending with a storage buffer, PBS-BN (PBS with 1% BSA and 0.05% sodium azide, Sigma-Aldrich). The particle solution was stored at 4°C until used (Bangs, 2008).

2.5 – Blood Sample Preparation

Human whole blood was obtained from Interstate Blood Bank; the sample was Type O with heparin anticoagulant, and was stored at 4°C until use. After 30 seconds of vortex mixing, the blood was aliquoted into ten separate vials, nine of which were spiked with the varying concentrations of HRP-2 antigen formed by serial dilution in section 2.3 – HRP-2 Antigen Preparation. The tenth vial served as the control, where 50mM PBS was used in place of HRP-2 antigen. The samples were then serially diluted in PBS to 10% and 1% of whole blood.

2.6– *Salmonella* Preparation

Salmonella enterica samples were obtained from Meridian Life Science and had an initial concentration of 7.9 colony-forming units (CFUs)/mL. Samples were cultured in a 90% brain heart infusion broth for 24 hours in order to reach a final concentration of

approximately 9 CFU/mL. The *Salmonella* sample was then serially diluted down to 1 CFU/mL, and added to the whole blood samples described in section 2.5 – Blood Sample Preparation. Additional nanoparticles were conjugated with polyclonal *Salmonella* antibodies according to the procedure described in section 2.4 – Nanoparticle Preparation.

2.7 – Experimental Procedure

2.7.1 – Blood Sample Optimization with *Salmonella* Target

The first objective of the experimental procedure was to determine the detection limit of pathogens in human whole blood. Due to the high cost of HRP-2 antigens, *Salmonella* target was substituted for these optimization experiments. *Salmonella* was chosen specifically due to being low-cost and readily available in our laboratory; although the size of live bacteria in *Salmonella* would be much larger than HRP-2 antigens, they would be useful in determining what was the minimum blood dilution required for pathogen detection in human blood. Whole blood samples with dilution factors of 10% and 1% were examined using 20 µL two-well slides using an Ocean Optics USB4000 fiber optic benchtop spectrometer. Ocean Optics Spectrasuite software for Windows, connected via USB cable to the spectrometer, was used to monitor the light scatter levels. The software displayed the amount of light scatter as an integer over a range of wavelengths, with region of interest lying between 640-660 nm. The Spectrasuite interface is shown in Figure 13.

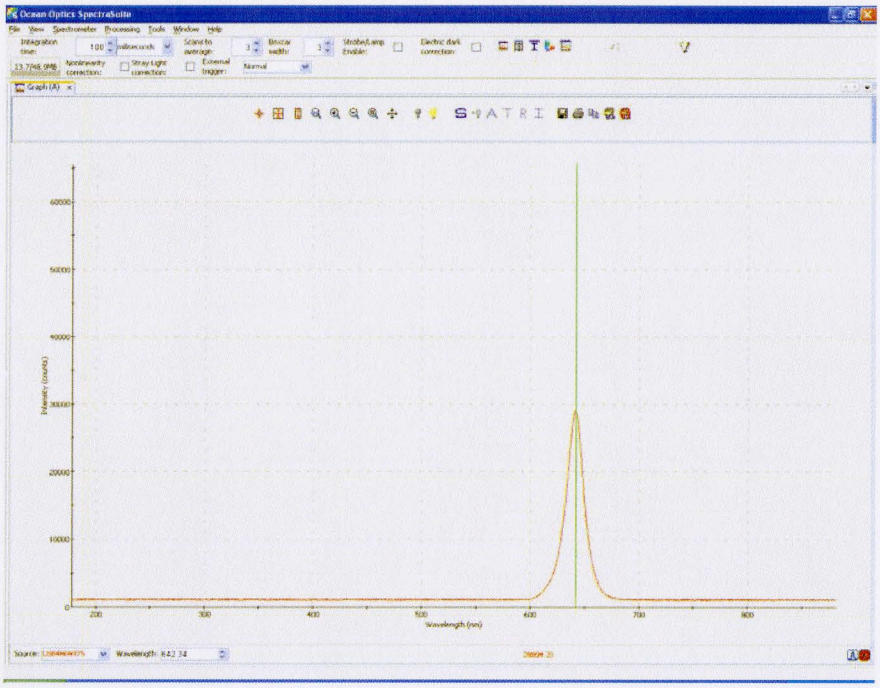

Figure 14 – Spectrasuite software for benchtop sprectrometer detection.

A 1:1 ratio of target to antibody conjugated particles was used for all experiments. Additionally, a polysorbate-80 nonionic surfactant was introduced to the samples just prior to detection in order to stabilize the nanoparticles (Tween-80, 0.02% mL/mL, pH 7, Sigma-Aldrich). For each 20 µL well, 14 µL PBS buffer was combined with 7 µL of diluted whole blood with *Salmonella* , 7 µL of nanoparticles, and 2 µL of surfactant for a total volume of 30 µL; this volume was chosen in order to mitigate the chance of air bubbles forming in the well . A 1.8x1.8 mm glass cover slip was placed over the well, which was then centered underneath the 640 nm light source; a photodiode underneath the well measured the amount of forward light scatter. The Spectrasuite software was used to determine the intensity of the forward light scatter in the

wavelength region of interest. Two additional control trials were performed: the positive control substituted 50mM PBS in for the diluted blood, and the negative control used nanoparticles without any antibody bound to them.

For all experiments, the blank is taken to be diluted whole blood in the absence of target; since each experiment is normalized to itself, the intensity change of each trial can be directly compared to another trial.

2.7.2 – Immunosensing of HRP-2 with Benchtop Detection System

The second experiment was designed to validate the detection of immunoagglutination of HRP-2 antigens in whole blood using the Y-channel microfluidic chip. Detection was again determined using the USB4000 spectrometer and the Spectrasuite software. Again using a 1:1 ratio of target to nanoparticles, 15 µL of 10% diluted whole blood with HRP-2 was added to one well of the Y-channel, while 15 µL of nanoparticles were added to the other well. Since HRP-2 was present in the whole, untreated blood, the concentration of HRP-2 was reduced by the same dilution factor as the blood. Just prior to detection, 2 µL of surfactant was added to the whole blood well, and a 1 mL syringe attached to the port at the end of the channel was used to draw the blood and particles into the central channel. An image of the experimental setup is shown in Figure 14. Since the purpose of this experiment was only to confirm the ability to detect HRP-2 in whole blood using the microfluidic chip, no additional trials were performed.

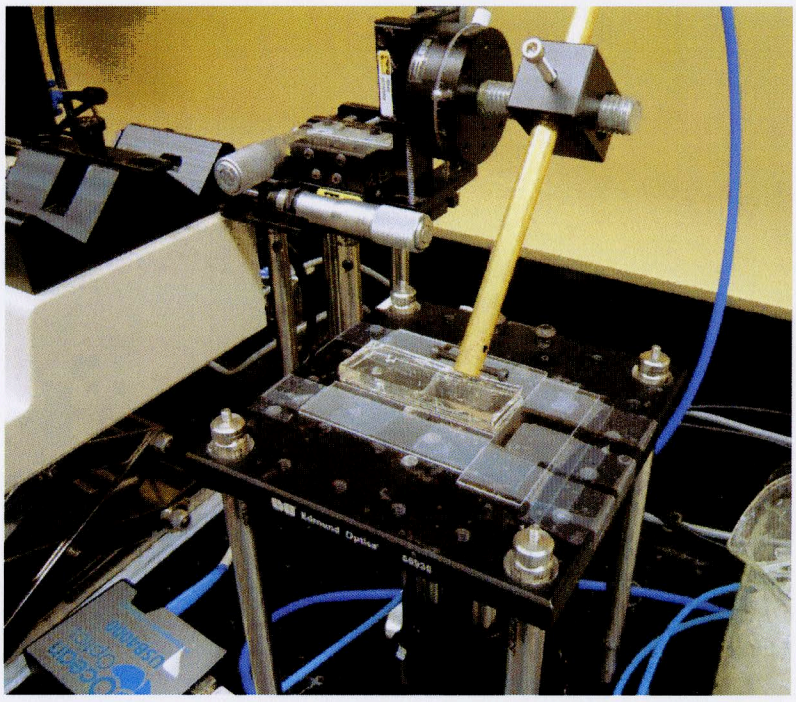

Figure 15 – Experimental setup for microfluidic chip validation.

2.7.3 – Immunosensing of HRP-2 with Handheld Device

The third experiment was designed to validate the detection of immunoagglutination of HRP-2 antigens using the handheld device. The experimental procedure was largely identical to the one described in Section 2.7.2, with the exception that the benchtop device was replaced by the handheld device. Bare 100 µm fiber optic cables were inserted into the waveguides, and microscope immersion oil was added to the waveguides until no air bubbles were present between the end of the cable and the central channel. The microfluidic chip and optic cables were then inserted into the removable test tray as shown in Figure 12.

A total of five trials were performed – three whole blood experiments and two controls. As in the previous experiments, the blood experiments detected for HRP-2 in 10% diluted whole blood, the PBS positive control detected for HRP-2 in 50 mM PBS, and the negative control detected for HRP-2 using nanoparticles that had no antibody bound to them.

2.7.4 – Specificity Tests

The final experiment was designed to verify that the chosen monoclonal antibody pair was specific to HRP-2 antigens. Using the same experimental procedure detailed in Section 2.7.3, nanoparticles bonded to the HRP-2 antibody pair were introduced to 10% whole blood with *Salmonella* target in the microfluidic chip and detected using the handheld device. Again, *Salmonella* was chosen specifically for its low cost and availability in the lab, not because it shares much in common with HRP-2 antigens.

Section 3

Results

3.1 – Blood Sample Optimization with *Salmonella* Target Results

The results of the experiments with *Salmonella* target using two-well slides and the benchtop spectrometer are shown in Figure 15. For all results, lines connecting the data points are included to aid in visualization.

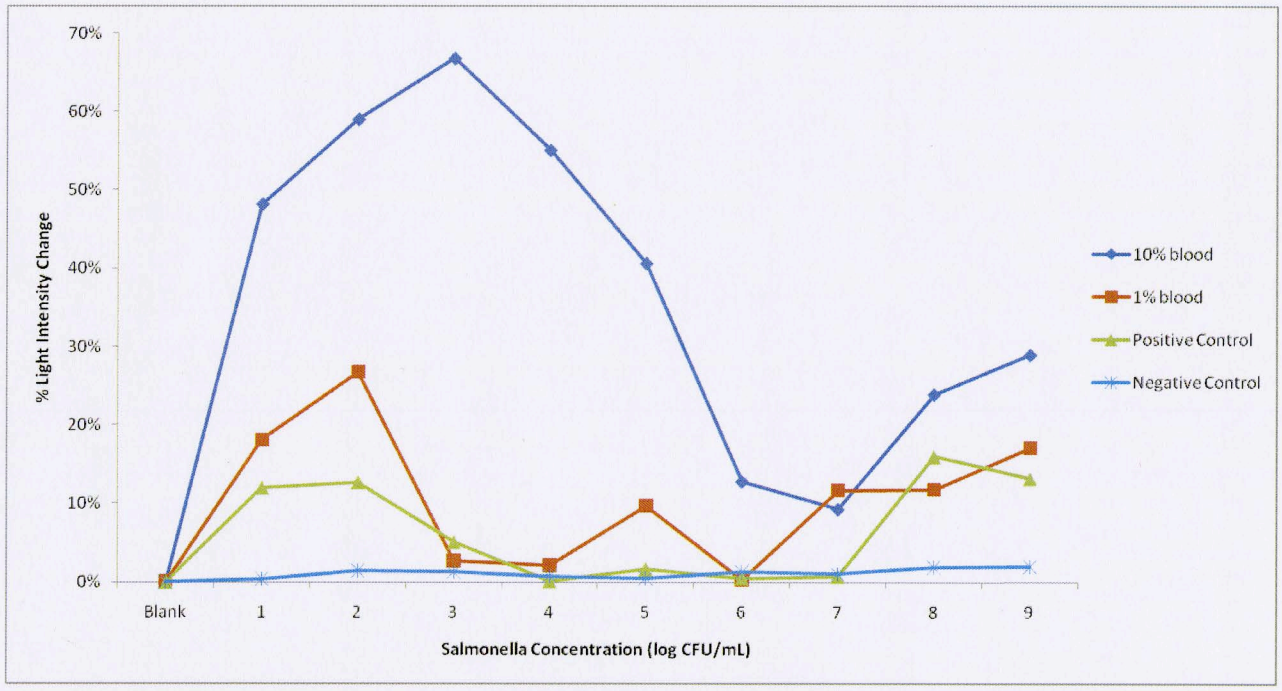

Figure 16 – Change in light scatter vs. *Salmonella* concentration in various whole blood dilutions, tested in a two-well slide using a benchtop spectrometer.

In 10% whole blood, a maximum intensity change of 66.8% was observed at a *Salmonella* concentration of 10^3 CFU/mL; in 1% blood, the maximum intensity change was 26.7% at 10^2 CFU/mL; in PBS, the maximum observed change was 12.6% at 10^2

CFU/mL. A linearly increasing trend was observed over at least two orders of magnitude for all trials; in 10% blood, this trend was observed over three orders of magnitude. For the positive control experiment using a PBS medium, a maximum signal change of 12.6% was observed at a *Salmonella* concentration of 10^2 CFU/mL; for the negative control experiment using particles without antibody attached, the maximum signal change was 2% at 10^9 CFU/mL with an average change of 1% over all concentrations.

3.2 – Immunosensing of HRP-2 with Benchtop Detection System Results

The results of the HRP-2 validation experiments in 10% whole blood with the microfluidic chip using the benchtop spectrometer are shown in Figure 16.

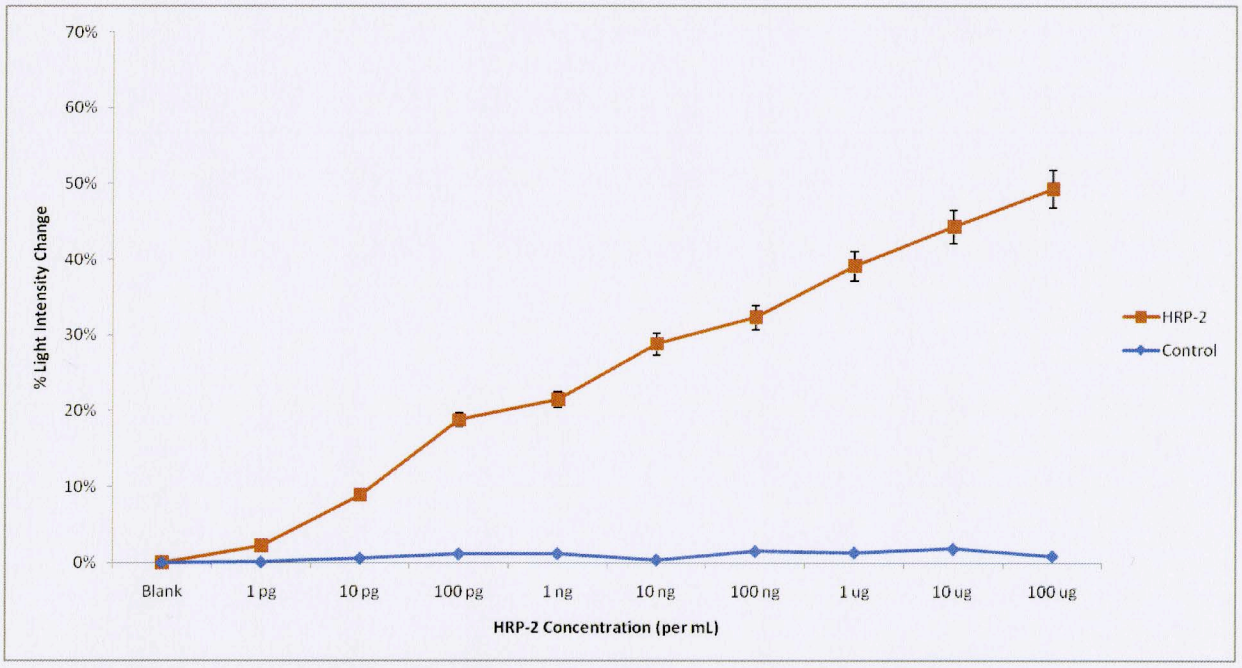

Figure 17 –Change in light scatter vs. HRP-2 concentration in 10% whole blood, tested in a microfluidic chip using the benchtop detection system. Standard error bars may be too small to be viewed for some data points.

A linearly increasing trend with an R^2 value of 0.9925 was observed over nine orders of magnitude, with a minimum intensity change of 2.2%, and a maximum change of 49.3%. The largest standard deviation was calculated to be 0.79% at 100 µg/mL with a standard error of 0.46%.

3.3 – Immunosensing of HRP-2 with Handheld Device Results

The results of the experiments with HRP-2 target in 10% whole blood using the microfluidic chip and handheld detection device are shown in Figure 17; the average of the three blood experiments with statistical analysis is shown in Figure 18.

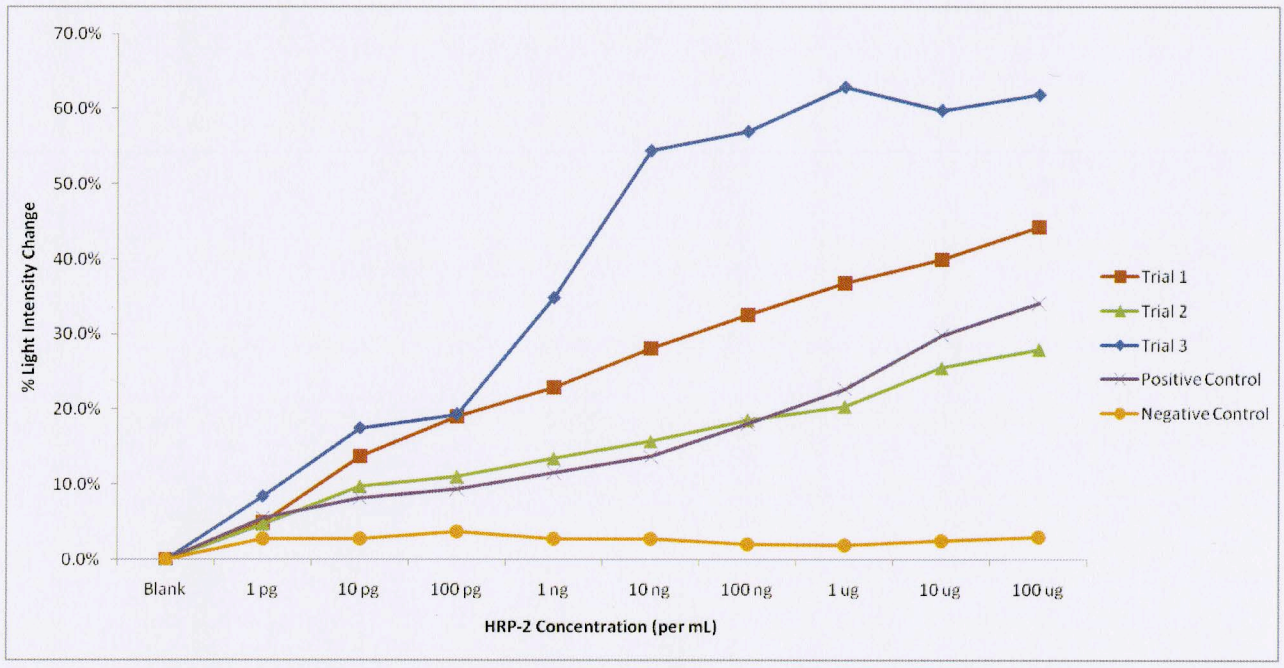

Figure 18 – Change in light scatter vs. HRP-2 concentration in 10% whole blood, tested in a microfluidic chip using the handheld device

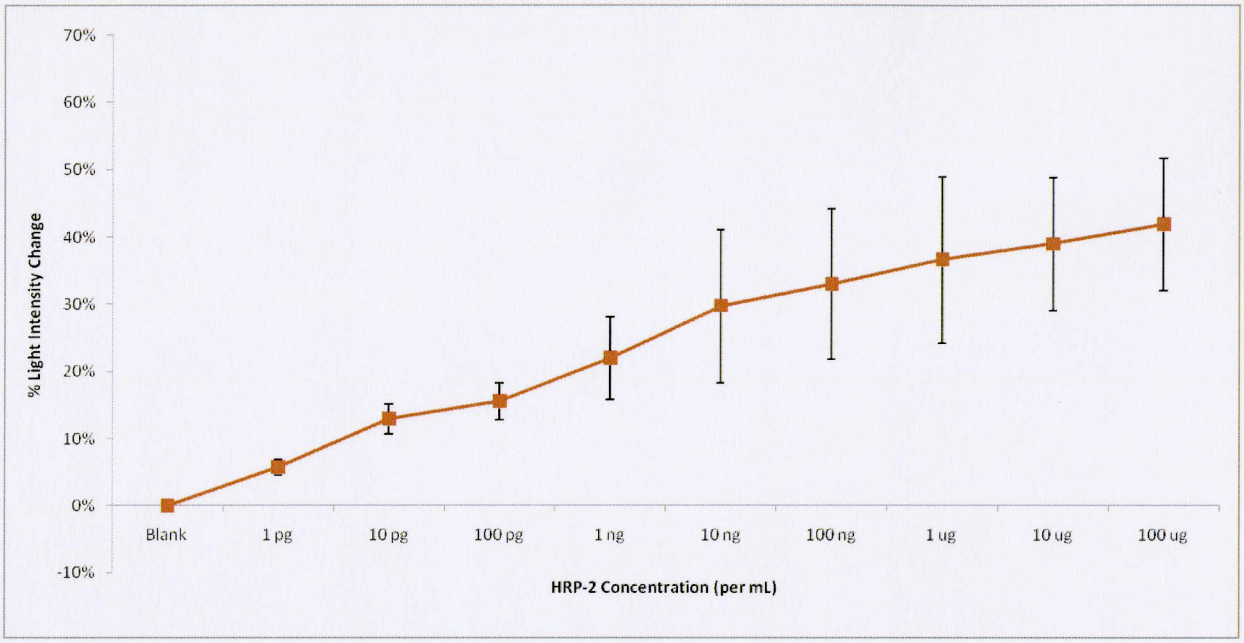

Figure 19– Average of all blood trials presented in Figure 17 with standard error bars.

All trials demonstrated a linear trend over nine orders of magnitude. The maximum observed signal change during Trial 1 was 44.3%, with a minimum change of 4.9% and an R^2 value of 0.9861; during Trial 2, the maximum change was 28%, and the minimum was 4.7% and an R^2 value of 0.9834; during Trial 3, the maximum change was 62.9%, and the minimum was 8.4% and an R^2 value of 0.9155. The largest standard deviation was calculated to be 21.4% at 1 µg/mL with a standard error of 12.37%. For the positive control experiment using a PBS medium, a maximum signal change of 26.7% was observed at an antigen concentration of 100 µg/mL, ; for the negative control experiment using particles without antibody attached, the maximum signal change was 3.7% at a concentration of 100 pg/mL, with an overall average change of 2.38%. The

largest standard deviation of 0.0.66% was observed at 10 µg/mL, with a standard error or 0.38%.

3.4 – Specificity Results

The results of the HRP-2 monoclonal antibody pair specificity tests are shown in Figure 20.

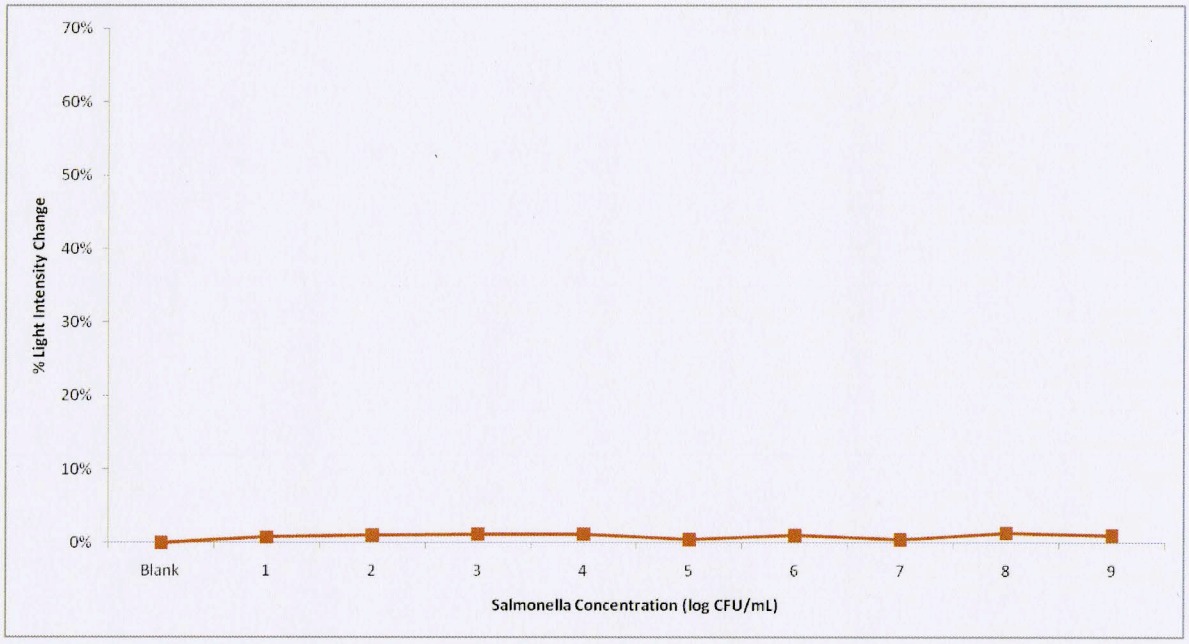

Figure 20 – HRP-2 specificity experiments with *Salmonella* target in a microfluidic chip using the handheld

detection device

A maximum signal change of 1.37% was observed at a *Salmonella* concentration of 10^8 CFU/mL, with an overall average change of 0.84%. The largest standard deviation of 0.42% was calculated at a concentration of 10^4 CFU/mL, with a standard error or 0.24%.

Section 4

Discussion

4.1 – Detection of Immunoagglutination in Human Whole Blood

Prior to validating the handheld's ability to detect for immunoagglutination, we had to first determine the optimal human whole blood preparation method. Preliminary tests showed that undiluted whole blood proved to be too protein-rich in order to determine whether scatter was a result of protein excess or immunoagglutination of the target to the nanoparticles. Thus, blood dilutions became necessary and dilutions as low as 0.01% were tested. Every dilution also resulted in an order of magnitude loss of antigen concentration; dilutions below 1% resulted in a 99% reduction in target concentration, leading to an excess of particles relative to antigens in the detection sample. Increased blood dilution factors also extend assay times, making the lowest detectable dilution factor ideal for short assay times. The purpose of administering the target pathogens to whole blood prior to dilution was to make the samples as clinically relevant as possible; introducing the diluted blood to the pathogens would result in artificially high detection limits.

As shown in Figure 16, immunoagglutination of *Salmonella* in blood dilutions of 10% and 1% were detectable, with the 10% dilution proving to be over 50% more sensitive than the 1% dilution. The control experiments were designed to ensure that increased light scatter was a result of specific immunoagglutination between the nanoparticles and *Salmonella* target, not increased antigen concentration or other

phenomena. There is a minimum of a 10% change in intensity between the lowest measured value of the 10% diluted blood and the highest measured value of the control blood without particles. Although control experiments weren't performed on the 1% diluted blood, there is at least a 2% intensity change difference between the lowest measured value of the 1% diluted blood and the highest measured value of the 10% control blood; this data indicates that the observed increase in light scatter is in fact the result of antibody-nanoparticle-target complex formation. The experiment involving nanoparticles with no bound antibody produced no greater than a 1% change from the lowest to highest *Salmonella* concentrations; this flat trend indicates that nanoparticles bound to polyclonal *Salmonella* antibodies are selectively binding to *Salmonella* target and not other proteins in the blood. It should be noted that the decreasing trend observed after 10^3 CFU/mL is an optical phenomenon also observed in previous studies using *E. coli* and *Salmonella*.

4.2 – Immunosensing of HRP-2 Antigens

The purpose of the benchtop testing of the microfluidic chip was to validate the chip as an effective testing environment and determine if the chosen HRP-2 antibody pair was capable of binding HRP-2 antigen. A linearly increasing change in scatter was observed over all concentrations of HRP-2, with a small standard deviation over the course of several trials. Although the benchtop spectrometer represents an idealized detection method due to being less prone to variation in output (as noted by a standard

deviation less than 1%), it verified that immunoagglutination of HRP-2 antigens to the nanoparticles was possible in diluted whole blood.

The results of the handheld testing closely resemble those of the benchtop tests, with increasing light scatter over the range of HRP-2 antigen concentrations with a detection limit of 1 pg/mL, albeit with a larger standard deviation. The specificity test showed that there was less than a 1% change in intensity throughout the range of *Salmonella* concentrations, with a maximum observed change of 1.37% from the blank, verifying that the HRP-2 antibodies do not cross-react with *Salmonella* target and demonstrating 100% specificity for this experiment.

It should be noted that the measured light scatter during Trial 3 was significantly higher than the values measured in Trials 1 and 2. This may be a result of build-up of blood proteins on the channel walls. Although the channels are designed to promote laminar flow, if blood cells were to bind to the channel walls, then light scatter would increase over the course of the experiment due to a buildup of blood cells. In order to mitigate channel wall contamination, the channels were washed with PBS after every blood trial. In order to verify that increased scatter was not due to build-up on the channel wall, the order of experiments for Trial 2 was reversed, such that the highest concentration of HRP-2 was tested first, and the lowest concentration was tested last. Since the same linear trend was present, it was determined that the blood had no short-term effects on the channel walls. However, the data from Trial 3 shows that the light scatter increased dramatically for HRP-2 concentrations above 1 ng/mL, contributing to

a relatively large standard deviation for concentrations between 10 ng/mL and 100 μg/mL. Thus, it is possible that the chip is only accurate for a finite number of trials before the channel wells either break down or begin to suffer from contamination. Since the microfluidic chips are designed to be disposable, this would not detract from the handheld's performance in the field as the chips would be disposed of after each experiment.

It should also be noted that the measured light scatter in the positive control PBS sample was no higher than in any of the blood samples; PBS represents the ideal sample environment, as it is theoretically clear and devoid of other molecules, making any light scatter the result of immunoagglutination only. However, since a majority of blood is composed of blood cells and albumin, we expect that overall scatter would be higher; the fact that light scatter remains relatively constant over increasing antigen concentration indicates that increased light scatter is a result of an increased number of antibody-nanoparticle-antigen complexes, not proteins in the blood. Further, the increased scatter caused by antigens in blood may also be due to the presence of human serum albumin, which is the most abundant of the human blood plasma proteins. A recent study by Kaminski et al revealed that albumin, which has been used in previous studies to mitigate nonspecific cell adhesion to target substrates, has a propensity to bind to unmodified polystyrene surfaces (Kaminski, 2011). Since the HRP-2 antibody pair only covers 30-50% of the nanoparticle surface, it is likely that albumin in the blood attaches to those unbound surfaces and stabilizes the particle, resulting in

increased binding to the HRP-2 target and ultimately, a higher degree of measured light scatter.

4.3 – Significance

4.3.1 – Comparison with Current Detection Methods

There are two primary advantages that the handheld has over current detection methods – decreased assay time and portability. As the majority of malaria occurrences are in sub-Saharan Africa, Asia, and South America, where proper testing facilities may be few and far between, the overall detection time is typically lengthened by several days to account for the time it takes to transport the sample to a test facility. Since the onset of symptoms due to *P. falciprum* can occur in less than a week from the time of infection, those days can mean the difference between mild symptoms and death. Hence, the ability to bring the detection device to the outbreak region is a significant leap forward for malaria detection, and can reduce assay times anywhere from a few days to a week.

The detection limit and the specificity of the handheld device is on par with blood smears, ELISA, and PCR. The detection limits of the various methods are summarized in Table 3. Note that all detection limits have been converted from trophozites/mL to pg/mL so that all methods could be directly compared. This was done using the assumption that the volume of a mature trophozite could be approximated as a sphere, that a trophozite's diameter is 15 μm, and that its density was 1 g/mL (3).

$$Density = \left(\frac{4}{3}\pi r^3\right) n \quad (3)$$

Where r is the diameter of the trophozite and n is the number of trophozites in one mL, as expressed in Section 1.2.

Table 3 – Detection method comparison

Method	Sensitivity (pg/mL)	Sensitivity (trophozites/mL)	Assay Time
Thick blood smear	88	50,000	1-8 hours
Thin blood smear	88000	50,000,000	1-8 hours
ELISA	32	18,000	2-3 hours
PCR	2	1,000	4-5 hours
Handheld device	1	500	5-8 minutes

The handheld demonstrated the lowest detection limit of all the various malaria detection methods; although obviously more sensitive than blood smear tests, the sensitivity of ELISA and PCR varies depending on the study, so the handheld is at the very least comparable to these two methods. However, the handheld is superior to both ELISA and PCR in terms of assay time; whereas the former methods require several hours to perform, a test on the handheld device can be performed in five minutes. The assay times in Table 3 do not reflect any additional time required to transport the blood samples from the draw site to the lab. While additional trials beyond this study would be needed in order to confirm the statistical relevance of the handheld's detection limit,

we can determine that the handheld is a viable method of detecting for *p. falciparum* parasites in human whole blood.

Potential issues with *P. falciparum* detection using the handheld device include the possibility of false positive as well as false negatives. Since this experiment tests for the presence of HRP-2 proteins in the blood and not live parasites, it could yield a false positive after a malaria infection has already been treated, as the protein levels will remain high in the blood even after the parasites have been removed. Further, there is evidence that not all *P. falciparum* parasites express HRP-2 (Ndao, 2004). Thus, this experiment would be unable to detect any such *P. falciparum* parasites, resulting in a false negative. In order to mitigate the chance of false negatives, further study would be required in order with live parasites in order to determine what other proteins they specifically express; targeting proteins in addition to HRP-2 may decrease specificity, but could eliminate the chance of missing an active infection.

4.3.2 – Applications

With comparable detection limits to the current malaria detection standards coupled and increased portability, the handheld device has potential applications in any area of the world in which is prone to malaria infection. The small form factor and battery could allow it to be taken into regions whose geography would limit the usefulness of other detection methods due to the amount of time required to travel to and from the regions, as blood samples can be affected by long transit times.

Additionally, since the device was able to detect both *Salmonella* and HRP-2 in blood samples, it could theoretically be modified to detect for a variety of pathogens by binding specific antibodies to the nanoparticles.

4.3.3 – Cost Analysis

A summary of the cost to replicate the handheld device is shown in Table 4.

Table 4 – Summary of handheld build cost.

Item	Vendor	Cost
Main circuit fabrication	Advanced Circuits	$350
Main circuit components	Digi-Key	$20
Arduino	Sparkfun	$30
LCD Display	Sparkfun	$18
Misc. electronics	Sparkfun	$30
Lithium-ion battery	Sparkfun	$40
Microfluidic chip	n/a	$0.50
ABS housing	PADT	$500
		Total - $988.50

The cost to replicate the device is just under $1000; however, the cost per unit could be reduced considerably through mass-production of the device, which would drive down the cost of the most expensive components (the main circuit board and the rapid-prototype housing) down by 80% or more.

Compared to the cost of other detection methods, with the exception of blood smears, the initial cost of creating a single handheld device is higher than a single ELISA

or PCR kit. Table 5 shows examples of the costs associated with the various malaria detection methods.

Table 5– Cost comparison of various malaria detection methods.

Method	Equipment Cost	Reagent Cost	Work Hours	Cost per Test
Blood smears	$1500-2000	$0	2	$40
ELISA	$22,000-29,000	$550	2	$46
PCR	$3500-6500	$425	4	$84
Handheld Device	$200-1000	$150	0.15	$5

As shown above, the cost of the handheld device is roughly double that of a PCR or ELISA kit specific to *P. falciparum*, but about half as expensive as a microscope for blood smears. However, the ELISA and PCR kits have a finite number of uses; since each kit contains a 96-well slide, a maximum of 96 tests can be administered per kit. Thus, for larger populations, the cost to purchase multiple kits will exceed the cost of a single handheld device, which has a lifespan of several years and only requires inexpensive PDMS chips for additional experiments. The cost per test was calculated by multiplying the number of work hours times by arbitrary rate of $20 (a reasonable hourly wage for a laboratory technician) and adding it to the reagent cost per test. The equipment costs were obtained from current market values; blood smears require a microscope, ELISA requires a plate reader, and PCR requires a thermocycler. Blood smear tests require no additional reagent, as the blood samples are simply placed on microscope slides for

analysis. For ELISA and PCR, 96-well kits are purchased which contain everything necessary for their respective tests. For the handheld device, the reagent cost only consists of purchasing antibodies and microfluidic chips; since only 7.6 μL are used for each set of particles, the cost of antibodies is nearly negligible as many tests can be performed with a single vial. The handheld device had both the lowest initial cost as well as the lowest cost per test, making it a cost-effective method for accurately detecting HRP-2 antigen in human blood.

4.4– Future Work

There are two major components which could benefit from future improvement – the electronics and the microfluidic chip itself. The main circuit board consists entirely of leaded, discrete components, which are typically reserved for non-sensitive applications due to the increased capacitance of the leads as well as the potential for mechanical failure. A switch to surface-mount components would increase the mechanical strength of the board considerably, while increasing overall electrical stability of the. Further, the size of the op-amp cascade could be decreased from six amplifiers to as few as two by switching to precision instrumentation amplifiers, such as the Texas Instruments INA128, which could also increase the stability of the voltage output. The orientation of the photodiode could also be adjusted for increased sensitivity; currently, it is set up in reverse-bias mode, which is optimized for speed at the cost of reduced sensitivity.

However, this additional speed is unnecessary for this particular circuit; forward-biasing the photodiode would increase sensitivity without any noticeable performance loss.

The main limitation of the Y-channel chip is that in order to maintain accurate results, the device must be recalibrated between experiments due to the single channel design; this increases the overall assay time, and increases the chance of user-error. An improved design would consist of two isolated channels, each with a unique LED/photodiode pair for detection. One channel would be used for the clinical sample, while the other would contain a control sample. This would allow the user to quickly determine the difference in light intensity change, as well as identify abnormalities with either of the samples.

Although the form factor of the handheld is significantly smaller than other detection systems, it's sized could be decreased further through merging all of the electronics onto a single, custom circuit board. As shown in Figure 8, a majority of the interior of the device is dedicated to the individual circuits and their interconnections; merging all of the circuits together with smaller, surface mount components could decrease the overall size of the device by 40% or more.

One issue that would need to be addressed prior to commercialization of the handheld device would be creating a long-term storage method for the antibody-conjugated particles. In the laboratory, the particles required storage at 4° C; however, in order to be a truly portable device, the particles would require transportation without the need for a refrigerator. One way to do this would be to lyophilize the nanoparticle-

antibody complexes prior to travelling to the test site; this would eliminate the need for a refrigerator, and only require a small cooler with dry ice in order to keep the particles stable.

Specificity tests against *Salmonella* were performed in order to gauge how well the chosen HRP-2 antibodies selectively bound to the HRP-2 antigens; however, since the *Salmonella* target consisted of full-sized bacteria, they have little in common with the recombinant HRP-2 antigens. Thus, more rigorous testing would need to be performed in order to validate the handheld device's specificity; this could be accomplished through testing for cross-reactions between HRP-2 antibodies and antigens from other *Plasmodium* species, such as HRP-1 and AMA1.

References

Desowitz, R. S. The Malaria Capers - More Tales of Parasites and People, Research and Reality. W.W. Norton & Company, New York, 1991.

Cox, F. E. (2010). History of the discovery of the malaria parasites and their vectors. *Parasites vectors, 3*(1), 5.

Heussler, V., Sturm, A., & Langsley, G. (2006). Regulation of host cell survival by intracellular *Plasmodium* and *Theileria* parasites. *Parasitology*, 132(Supp), S53.

Miller, L.H., Baruch, D.I., Marsh, K., & Doumbo, O.K. (2002). The pathogenic basis of malaria. *Nature,* 415, 673-679.

Tripet, F., Aboagye-Antwi, F., & Hurd, H. (2008). Ecological immunology of mosquito-malaria interactions. *Trends in Parasitology, 24,* 5, 219-227.

Pouvelle, B., Buffet, P. A., Lépolard, C., Scherf, A., & Gysin, J. (January 2000). Cytoadhesion of Plasmodium falciparum ring-stage-infected erythrocytes. *Nature Medicine, 6,* 11, 1264-8.

Pouniotis, D. S., Proudfoot, O., Minigo, G., Hanley, J. L., & Plebanski, M. (2004). Malaria parasite interactions with the human host. *Journal of Postgraduate Medicine, 50,* 1.

Bain, B. J. (January 2009). Fatal Plasmodium falciparum infection. *American Journal of Hematology, 84,* 2.

World Health Organization (April 2011). Malaria. Retrieved from http://www.who.int/topics/malaria/en/. Accessed on 3 Aug 2011.

Center for Disease Control (February 2010). About Malaria. Retrieved from http://www.cdc.gov/malaria/about/index.html. Accessed on 3 Aug 2011.

Warhurst D.C., Williams J.E. (1996). Laboratory diagnosis of malaria. *J Clin Pathol* 49 (7): 533–38.

Moody, A. H., & Chiodini, P. L. (2000). Methods for the detection of blood parasites. *Clinical and Laboratory Haematology, 22,* 4, 189-201.

Stauffer, W. M., Boulware, D. R., Cartwright, C. P., Hanson, K. L., Olson, D. A., Juni, B. A., Taylor, C. M., ... Rosenblatt, J. E. (September 15, 2009). Diagnostic

performance of rapid diagnostic tests versus blood smears for malaria in US clinical practice. *Clinical Infectious Diseases, 49,* 6, 908-913.

Keas, B. E. (1999). Microscopy – *Plasmodium* Species, retrieved from https://www.msu.edu/course/zol/316/psppscope.htm. Accessed on 5 Aug 2011.

Crowther, J. R. (2001). *The ELISA guidebook*. Totowa, NJ: Humana Press.

Sure Bio-Diagnostics (2009). Infectious Diseases – Malaria. http://www.surebio.org/infectous.html. Accessed on 4 Aug 2011.

Johnston, S. P., Pieniazek, N. J., Xayavong, M. V., Slemenda, S. B., Wilkins, P. P., & da, S. A. J. (January 2006). PCR as a confirmatory technique for laboratory diagnosis of malaria. *Journal of Clinical Microbiology, 44,* 3, 1087-9.

Mangold, K. A., Manson, R. U., Koay, E. S., Stephens, L., Regner, M., Thomson, R. B. J., Peterson, L. R., & Kaul, K. L. (2005). Real-time PCR for detection and identification of Plasmodium spp. *Journal of Clinical Microbiology, 43,* 5, 2435-40.

Gella, F. J., Serra, J., & Gener, J. (1991). Latex agglutination procedures in immunodiagnosis. *Pure and Applied Chemistry, 63,* 8, 1131-1134.

Molina Bolívar, J. A., & Galisteo González, F. (2005). Latex Immunoagglutination Assays. *Journal of Macromolecular Science, Part C: Polymer Reviews, 45,* 1, 59-98.

Kerker, M. (1969). *The scattering of light and other electromagnetic radiation*. New York: Academic

Nave, R. (2005). Mie Scattering, retrieved from http://hyperphysics.phy-astr.gsu.edu/hbase/atmos/imgatm/mie.gif . Accessed 2 Aug 2011.

Oosterbroek, R. E., & Berg, A. (2003). *Lab-on-a-chip: Miniaturized systems for (bio)chemical analysis and synthesis*. Amsterdam: Elsevier

Kwon, H.-J., Dean, Z. S., Angus, S. V., & Yoon, J.-Y. (2010). Lab-on-a-Chip for Field Escherichia coli Assays: Long-Term Stability of Reagents and Automatic Sampling System. *Jala - Journal of the Association for Laboratory Automation, 15,* 3, 216-223.

Heinze, B. C., Gamboa, J. R., Yoon, J.-Y., Kim, K., & Song, J.-Y. (2010). Microfluidic immunosensor with integrated liquid core waveguides for sensitive Mie scattering

detection of avian influenza antigens in a real biological matrix. *Analytical and Bioanalytical Chemistry, 398,* 6, 2693-2700.

Heinze, B. C., & Yoon, J. Y. (2011). Nanoparticle immunoagglutination Rayleigh scatter assay to complement microparticle immunoagglutination Mie scatter assay in a microfluidic device. *Colloids and Surfaces B: Biointerfaces, 85,* 2, 168-173.

You, D.J., Geshell, K.J., & Yoon, J-Y. (2011). Direct and sensitive detection of foodborne pathogens within fresh produce samples using a field-deployable handheld device. *Biosensors and Bioelectronics*, Article in Press.

Kwon, H.-J., Heinze, B. C., Yoon, J.-Y., Lee, C.-H., Choi, E.-J., & Song, J.-Y. (November 01, 2010). Optofluidic device monitoring and fluid dynamics simulation for the spread of viral pathogens in a livestock environment. *Journal of Environmental Monitoring, 12,* 11, 2138-2144.

Meridian Life Science, Specification Sheet #R01478: *P. Falciparum* HRP-2, Recomb (2011). https://meridianlifescience.com/bioSpecs/R01478.pdf. Accessed on 19 Jul 2011.

Kakkilaya, B. S. (2003). Rapid Diagnosis of Malaria. *Laboratory Medicine, 34,* 8, 602-608.

Meridian Life Science, Specification Sheet #C01584M: Monoclonal Antibody to *P. Falciparum* HRP-2, (2011). https://meridianlifescience.com/bioSpecs/CO1584M.pdf. Accessed on 19 Jul 2011.

Yoon, J.-Y. (2008). Latex Immunoagglutination Assay in Lab-on-a-Chip. *Biological Engineering, 1,* 1, 79-94.

Bangs Laboratories, Tech Note #204: Absorption to Microspheres. Bangs Laboratories, Fis 2008. http://www.bangslabs.com/files/bangs/docs/pdf/204.pdf. Accessed 24 June 2011.

Kaminski, J., & Kolos, R. (2011). Albumin adsorption on unmodified and sulfonated polystyrene surfaces, in relation to cell-substratum adhesion. *Colloids and Surfaces B: Biointerfaces, 84,* 2, 536-544.

Ndao, M., Bandyayera, E., Kokoskin, E., Gyorkos, T. W., MacLean, J. D., & Ward, B. J. (2004). Comparison of blood smear, antigen detection, and nested-PCR methods for screening refugees from regions where malaria is endemic after a malaria outbreak in Quebec, Canada. *Journal of Clinical Microbiology, 42,* 6, 2694-700.